MOLECULAR AND CELLULAR BIOLOGY, Feb. 2003, p. 916–922 Vol. 23, No. 3
0270-7306/03/$08.00+0 DOI: 10.1128/MCB.23.3.916–922.2003

The Absence of Mitochondrial Thioredoxin 2 Causes Massive Apoptosis, Exencephaly, and Early Embryonic Lethality in Homozygous Mice

Larisa Nonn, Ryan R. Williams, Robert P. Erickson, and Garth Powis*

Arizona Cancer Center, University of Arizona, Tucson, Arizona 85714-5024

Received 13 September 2002/Returned for modification 2 October 2002/Accepted 7 November 2002

Thioredoxin 2 (Trx-2) is a small redox protein containing the thioredoxin active site Trp-Cys-Gly-Pro-Cys that is localized to the mitochondria by a mitochondrial leader sequence and encoded by a nuclear gene (*Trx-2*). Trx-2 plays an important role in cell viability and the regulation of apoptosis in vitro. To investigate the role of Trx-2 in mouse development, we studied the phenotype of mice that have the *Trx-2* gene silenced by mutational insertion. Homozygous mutant embryos do not survive to birth and die after implantation at Theiler stage 15/16. The homozygous mutant embryos display an open anterior neural tube and show massively increased apoptosis at 10.5 days postcoitus and are not present by 12.5 days postcoitus. The timing of the embryonic lethality coincides with the maturation of the mitochondria, since they begin oxidative phosphorylation during this stage of embryogenesis. In addition, embryonic fibroblasts cultured from homozygous *Trx-2*-null embryos were not viable. Heterozygous mice are fertile and have no discernible phenotype visible by external observation, despite having decreased *Trx-2* mRNA and protein. These results show that the mitochondrial redox protein Trx-2 is required for normal development of the mouse embryo and for actively respiring cells.

The mitochondria are a critical site of reactive oxygen species (ROS) production within the cell. The electron transport chains within the mitochondria consume oxygen to produce water and cellular energy in the form of adenosine triphosphate. During this process of oxidative phosphorylation between 0.4 and 4% of the consumed oxygen is released in the mitochondria as ROS (3). Regulated ROS production is involved in receptor mediated cell signaling pathways, transcriptional activation, and normal cell proliferation (13, 25). ROS production is essential for normal mouse embryogenesis, and an increase in ROS of specific cells mediates the apoptosis that is required for cell elimination during embryonic morphogenesis (23).

If the redox balance of the cell is compromised, increased ROS production can cause detrimental oxidative damage to biological molecules. Aberrant increases in ROS within the mitochondria can induce apoptosis by causing the release of proapoptotic factors, including cytochrome *c* and apoptosis-inducing factor, via the opening of a nonselective pore (19, 27, 33). ROS-induced oxidative damage to the mitochondria has been implicated in aging and the pathology of a number of degenerative diseases (31).

The mitochondria contain antioxidant defenses that protect against ROS-induced damage, including manganese superoxide dismutase (MnSOD/SOD-2) (18), mitochondrial glutaredoxin (Grx2a) (11), glutathione/phospholipid hydroperoxide glutathione peroxidase (GSH/PHGPX [GPX4]) (16), catalase (22), and the thioredoxin 2 (Trx-2) system (21). The Trx-2 system, Grx2a, and MnSOD are mitochondrion-specific proteins, whereas GSH/PHGPX and catalase are present in other parts of the cell (11, 16, 18, 21, 22). In the MnSOD knockout mouse, the neonates die by age 10 days of neurodegeneration and dilated cardiomyopathy (18).

The Trx-2 (Trx-2 in mice; TRX-2 in humans) system includes Trx-2, mitochondrial thioredoxin reductase 2 (TrxR-2), and mitochondrial peroxiredoxin 3 (Prdx-3) (6, 7, 20, 26). Trx-2 is a member of the thioredoxin (Trx) family of small redox proteins that contain a conserved active site of Trp-Cys-Gly-Pro-Cys-Lys (26). The active-site cysteines of thioredoxins function to maintain protein thiols in a reduced state by becoming oxidized themselves. TrxR-2 regenerates Trx-2 by reducing the oxidized active site cysteines (20). Prdx-3 is a thioredoxin peroxidase that utilizes Trx-2 as an electron donor for the reduction of hydrogen peroxide (5). Trx-2, TrxR-2, and Prdx-3 proteins are each encoded in the nuclear genome and contain a mitochondrial leader sequence that is cleaved off after import of the protein into the mitochondria. The mitochondrial Trx-2 system is ubiquitously expressed, but it is found at the highest levels in the metabolically active tissues of the heart, brain, and liver (5, 20, 26).

Recent studies have shown that Trx-2 overexpression in vitro can protect the cell against *t*-butylhydroperoxide and etoposide-induced apoptosis, as well as increasing the mitochondrial membrane potential ($\Delta\Psi$) (8, 9). In addition, cells deficient in Trx-2 display increased cellular ROS and apoptosis (28).

We have examined the role of the Trx-2 system in mammalian development by generating a mouse deficient in Trx-2. The *Trx-2*$^{+/-}$ heterozygous mice appeared normal even though they displayed decreased levels of Trx-2, whereas early embryonic lethality was seen in the *Trx-2*$^{-/-}$ homozygous embryos.

* Corresponding author. Mailing address: Arizona Cancer Center, University of Arizona, 1515 N. Campbell Ave., Tucson, AZ 85724-5024. Phone: (520) 626-6408. Fax: (520) 626-4848. E-mail: gpowis@azcc.arizona.edu.

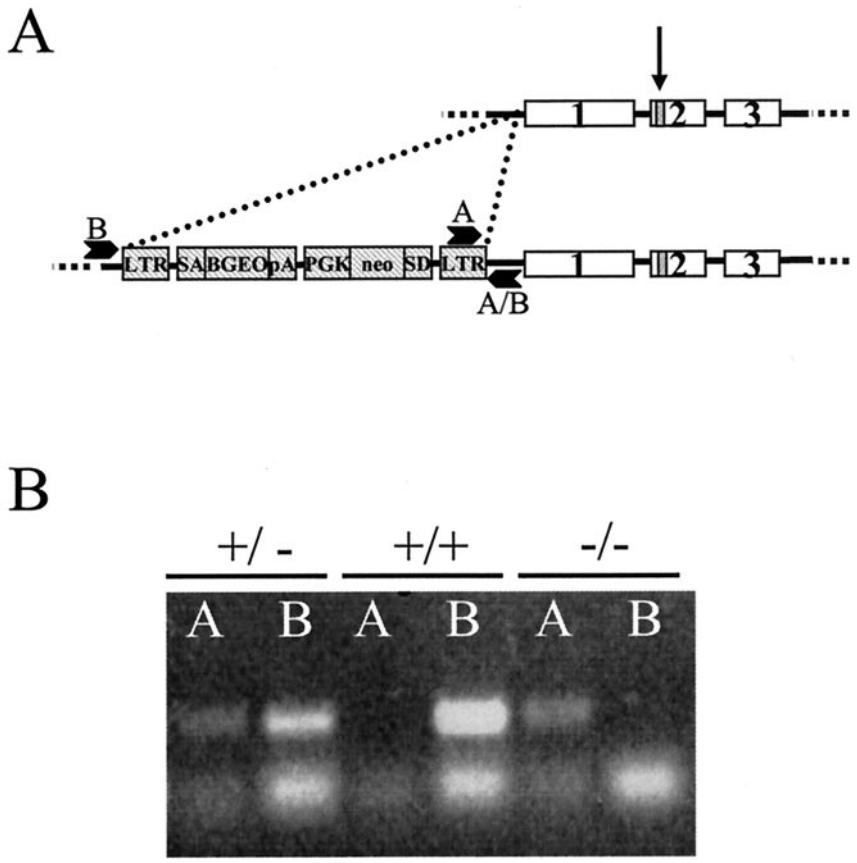

FIG. 1. Disruption of mouse *Trx-2*. (A) Diagram showing the three exons of the *Trx-2* locus (with an arrow indicating the location of active-site cysteines) (not drawn to scale), the retroviral insertion of LTR-SA-BGEO-pA-PGK-neo-SD-LTR2 (hatched boxes) 351 bp upstream of exon 1, and the location of genotyping PCR primers A and B. (B) Genotyping of mouse DNA by two PCRs: one PCR for the mutant allele (lanes A) and one PCR for the wild-type allele (lanes B). *Trx-2*$^{+/-}$ mice are positive for both A and B, *Trx2*$^{+/+}$ (wild-type) mice are positive only for B, and *Trx-2*$^{-/-}$ mice are positive only for A. The top bands are the specific PCR products, and the bottom bands present in all of the lanes are the primer dimer.

MATERIALS AND METHODS

Chemicals and reagents. All chemicals and reagents were supplied by Sigma-Aldrich (St. Louis, Mo.) unless otherwise stated.

Generation of *Trx-2*$^{+/-}$ heterozygous mice. Founder mice were created by Lexicon Genetics (The Woodlands, Tex.) and developed by gene trapping by using random insertional mutagenesis with retroviral vector VICTR24 as described by Zambrowicz et al. (32). VICTR24 was generated by cloning a sequence acquisition component and a mutagenic component into the pGen supexpression vector, followed by packaging by GP+E86 cells. The acquisition component consists of phosphoglycerate kinase 1 promoter (PGK) fused to the neomycin resistance gene, followed by a synthetic consensus splice donor sequence (PGK-neo-SD), and the mutagenic component is a splice acceptor sequence fused to a colorometric marker, followed by a polyadenylation sequence (SA-bgeo-pA). Embryonic stem cells were retrovirally infected with VICTR24 and clonally selected. The presence of only one gene copy of the mutational insertion was verified by quality control, and the sequence of the trapped gene was obtained for each clone by 3′ rapid amplification of cDNA ends. The mouse *Trx-2* cDNA sequence was used to screen the Lexicon OmniBank library database of disrupted genes (http://www.lexgen.com). Clone OST69169, in which the mutational insertion is 301 bp upstream of *Trx-2* exon 1, was utilized to prevent transcription of *Trx-2*. The embryonic stem cells were injected into C57BL/6 blastocysts and implanted into pseudopregnant females. Chimeric pups were bred to generate heterozygous offspring.

Genotyping. Mice were maintained on NIH-31 modified irradiated rat and mouse chow (Harlan Techlad, Indianapolis, Ind.) and bottled water ad libitum. Mice were tail tipped and ear tagged at 3 weeks. DNA was extracted by using a DNeasy kit (Qiagen, Valencia, Calif.). For genotyping of formalin-fixed and paraffin-embedded embryos, embryonic tissue was scraped from unstained sections and deparaffinized prior to DNA extraction with the DNeasy kit. Genotyping was done by using two PCRs. One PCR for the insert was performed with a 5′ primer within the LTR2 insertion (5′-AAATGGCGTTACTTAAGCTAG CTTGC-3′) and a 3′ primer in chromosome 15 downstream of the insertion (5′-GGCATGCAATAGGAAGTCACAC-3′). A second PCR was performed with a 5′ primer in chromosome 15 upstream of the insertion (5′-CCTTCTAA CTTAACGTCTATTCAGT-3′) and a 3′ primer in chromosome 15 downstream

TABLE 1. Offspring genotypes from heterozygous matings

DNA source[a]	Total no. of zygotes	No. with genotype:			No. of resorbing embryos
		+/+	+/−	−/−	
3-wk-old pup	127	42	81	0	NA
Embryo					
12.5 dpc	24	7	9	0	8
10.5 dpc	33	8	13	2	10
9.5 dpc	32	10	15	5	2
8.5 dpc	6	2	3	1	0
9.5-dpc MEFs	20	4	11	5[b]	NA

[a] MEFs, mouse embryo fibroblasts.
[b] *Trx-2*$^{-/-}$ mouse embryo fibroblasts were not viable.

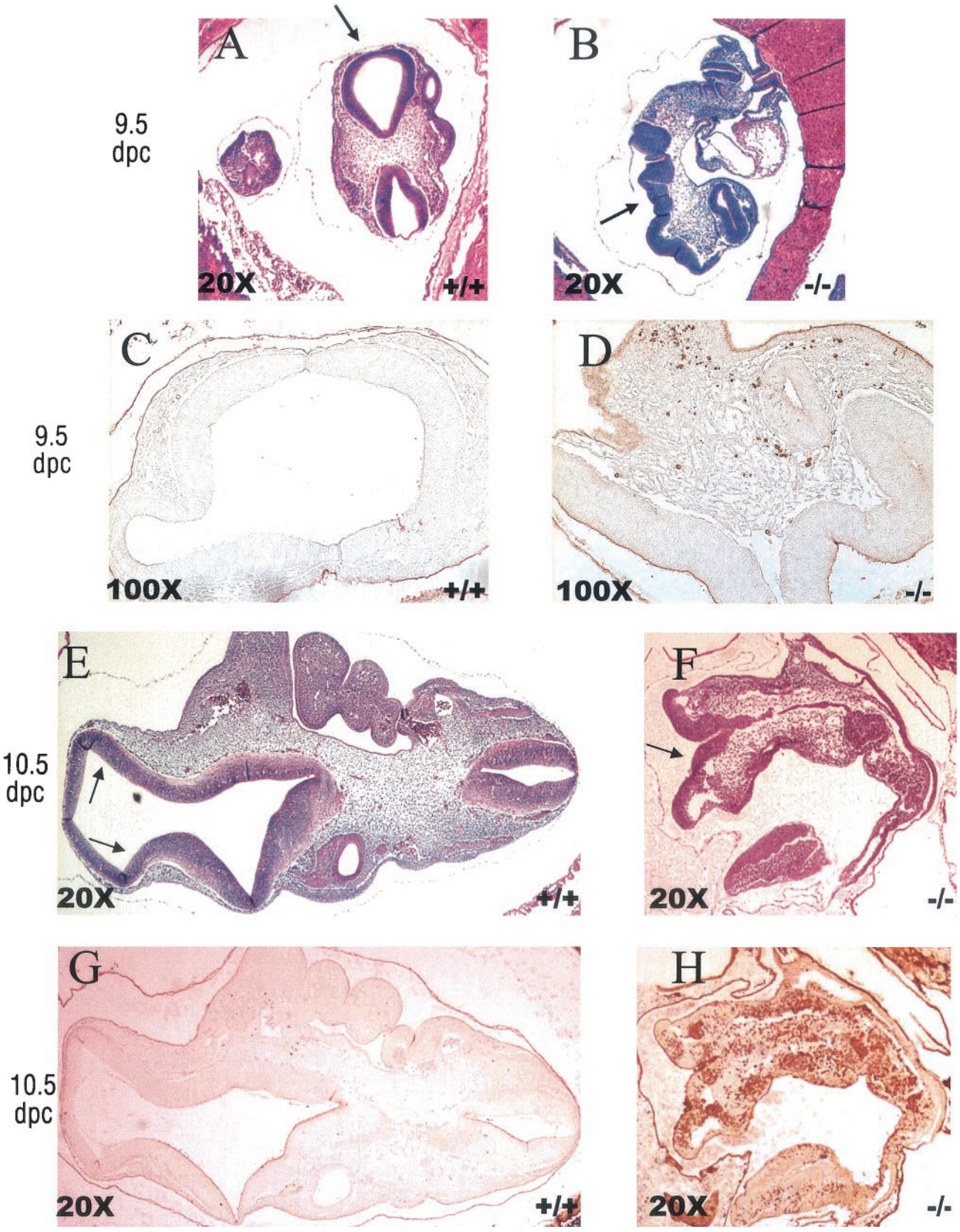

FIG. 2. Anterior neural tube defect and increased apoptosis in homozygous *Trx-2*$^{-/-}$ mice at 9.5 and 10.5 dpc (representative embryos and images). Aberrant anterior neural tube closure in *Trx-2*$^{-/-}$ embryo, indicated by arrows, was compared to the wild-type embryo by hemotoxylin and eosin staining of paraffin-embedded embryos at 9.5 dpc (A and B) and at 10.5 dpc (E and F). In panels C and D are shown increased

of the insertion (5′-GGCATGCAATAGGAAGTCACAC −3′). To aid in primer design, the LTR2 5′ and chromosome 15 flanking sequences were provided by Lexicon Genetics. PCR products were visualized by using agarose gel electrophoresis and staining with ethidium bromide.

Timed pregnancies. Female heterozygous mice, 6 to 10 weeks of age, were bred to heterozygous males. Pregnant females were sacrificed by cervical dislocation 12.5, 10.5, 9.5, and 8.5 days after the day of observing a vaginal plug. Uteri and embryos were removed for genotyping, Western blotting, or immunohistochemistry.

Mouse embryo fibroblasts. Embryos from a heterozygous mating were collected at 9.5 days postcoitus (dpc). Embryos were dissected from deciduum and individually incubated in trypsin for 5 min at 37°C. Cells were pipetted up and down, followed by two washes with phosphate-buffered saline. Small samples were reserved for DNA preparation and genotyping. Cells were plated in high-glucose Dulbecco modified Eagle medium supplemented with fetal bovine serum (20%), L-glutamine (2 μM), sodium pyruvate (1 mM), penicillin (50 IU/ml), and streptomycin sulfate (50 μg/ml) and then maintained at 37°C in 5% CO_2.

Antibody generation. TRX-2 was fused to maltose-binding protein by cloning into the pMAL prokaryotic expression vector (Invitrogen, Carlsbad, Calif.). Recombinant TRX-2/maltose-binding protein was expressed in *Escherichia coli*, purified by using a maltose column, and injected into 8-week-old male New Zealand White rabbits (Jackson Laboratories, Bar Harbor, Maine) to generate polyclonal antisera. Rabbit polyclonal antisera to a unique peptide sequence from ΔTRXR-2 and to a unique peptide sequence from PRDX-3 (SPAA SKEYFQKVNQ; Alpha Diagnostic, San Antonio, Tex.) were generated in a similar manner. These polyclonal antibodies to TRX-2, TRXR-2, and PRDX-3 all cross-reacted with the mouse proteins.

Mitochondrion isolation. Hepatic mitochondria were isolated by a modification of the method of Bustamante et al. (4). Briefly, mice were sacrificed by carbon dioxide asphyxiation, and their livers were removed. The livers were minced on ice, followed by homogenization with a Teflon pestle for six strokes in ice-cold MSH buffer (250 mM mannitol, 75 mM sucrose, 5 mM HEPES; pH 7.4) with 1 mM EDTA. The homogenates were immediately centrifuged for 10 min at 600 × *g* and 4°C; the supernatant was then transferred to a prechilled tube and centrifuged for 15 min at 6,800 × *g* and 4°C. The pellet was resuspended in ice-cold MSH buffer and centrifuged for 10 min at 600 × *g* and 4°C. The supernatant was centrifuged for 15 min at 6,800 × *g* and 4°C, and the mitochondrial pellet was resuspended in MSH buffer for electrophoresis and Western blot analysis (100 μg). Protein was quantified by using the Bio-Rad protein reagent (Bio-Rad, Hercules, Calif.).

Western blot analysis of mouse tissues. Heterozygous and wild-type mice at 6 to 10 weeks of age were sacrificed by cervical dislocation. Brain, liver, heart, lung, and kidney tissues were excised and placed in ice-cold lysis buffer (0.5% Nonidet P-40, 0.5% sodium deoxycholate, 50 mM NaCl, 1 mM EDTA, 1 mM $NaVO_3$, 50 mM HEPES [pH 7.5], 1 mM phenylmethylsulfonyl fluoride). Tissue samples were homogenized on ice with a PowerGen 35 (Fisher Scientific, Pittsburgh, Pa.). The tissue lysates were snap-frozen in a dry-ice ethanol bath and then thawed on ice. Lysates were cleared by centrifugation (10,000 × *g*) for 15 min at 4°C. Protein was quantified by using Bio-Rad protein reagent. Cleared tissue lysate (20 μg) was loaded onto a 10% NuPAGE gel (Invitrogen). The proteins were separated by electrophoresis and then transferred to polyvinylidene difluoride membrane (NEN, Boston, Mass.). Antibodies used in Western blotting were anti-TRX-2, TRXR-2, or PRDX-3 rabbit polyclonal antisera, anti-human MnSOD monoclonal antibody (Upstate Biochemicals, Lake Placid, N.Y.), and anti-bovine catalase rabbit polyclonal antibody (Rockland, Gilbertsville, Pa.), followed by the addition of horseradish peroxidase-conjugated anti-rabbit or anti-mouse secondary antibody. The results were visualized by Western Lightning chemiluminescence (NEN), followed by autoradiography.

RNA purification and Northern blot analysis. Liver total RNA was extracted by using Trizol Reagent (Invitrogen) and the PowerGen 35 homogenizer. Poly(A) RNA was purified from 500 μg of total RNA by using Oligotex beads (Qiagen). Poly(A) RNA (2 μg) was separated by electrophoresis on a 1.2% agarose gel, and RNA was transferred to nitrocellulose (Osmonics) for Northern blot analysis. cDNA probes were radiolabeled with [α-^{32}P]dCTP (NEN) by using the random prime labeling kit (Invitrogen). Blots were hybridized with radiolabeled probes overnight at 42°C in UltraHyb buffer (Ambion, Austin, Tex.). Nonspecific probe was removed by a series of washes. Northern blots were visualized by using autoradiography and a Molecular Dynamics PhosphorImager (Amersham Biosciences, Piscataway, N.J.) and then quantified by using ImageQuant software.

Immunohistochemistry. Embryos from 12.5-, 10.5-, 9.5-, and 8.5-dpc pregnant females were fixed in 4% formaldehyde in phosphate-buffered saline for 24 h prior to being routinely processed and embedded in paraffin. Tissues were serially sectioned at 4 μm and deparaffinized through xylene and graded alcohols prior to blocking. Sections were incubated with mouse anti-caspase-3 (Trevigen, Gaithersburg Md.) for 32 min at 42°C on a Ventana ES (Ventana Medical Systems, Tucson, Ariz.) automated slide stainer and then visualized by using the basic DAB detection kit (Ventana Medical Systems). Stained slides were dehydrated through graded alcohols and xylene prior to coverslipping. Certain sections were stained with a modified Harris' hematoxylin and eosin as morphological references.

RESULTS AND DISCUSSION

Lethality of Trx-2-deficient embryos and fibroblasts. Trx-2 is encoded by a single nuclear gene on mouse chromosome 15 (A. Miranda-Vizuete, A. Gustaffsson, and G. Spyrou, NCBI database entry MMU85089, 1997 [unpublished data]). Disruption of *Trx-2* transcription was achieved by the retroviral insertion of a gene trap 301 bp upstream of exon 1 (Fig. 1A). A single copy of the insertion was previously verified in the embryonic stem cells prior to microinjection by using Quality Control from Lexicon. Genotyping of the offspring was performed by using two PCRs (Fig. 1B). One PCR for the insert used a 5′ primer within the LTR2 insertion and a 3′ primer in chromosome 15 downstream of the insertion. A second PCR used a 5′ primer in chromosome 15 upstream of the insertion and a 3′ primer in chromosome 15 downstream of the insertion. The insertion did not cause an externally discernible phenotype in the heterozygous *Trx-2*$^{+/-}$ mice, whereas the homozygous Trx-2-null *Trx-2*$^{-/-}$ mice did not survive to birth (Table 1).

To determine the timing of the lethality during embryogenesis, embryos were collected from heterozygous matings at 12.5, 10.5, 9.5, and 8.5 dpc. The embryos were genotyped by PCR on DNA from embryonic tissue scraped off of unstained sections to determine the presence of mice deficient in *Trx-2* (Table 1). At 12.5 dpc, we observed normal embryos as well as embryos at various stages of resorption, and none of the normal embryos were genotyped as homozygous *Trx-2*$^{-/-}$ (Table 1). Homozygous *Trx-2*$^{-/-}$ embryos were observed in the 8.5-, 9.5-, and 10.5-dpc pregnant mice. At 8.5 dpc, the embryos did not have features that distinguished their genotype, and they all appeared normal regardless of the genotype (data not shown). By 9.5 dpc the *Trx-2*$^{-/-}$ embryos displayed an open anterior neural tube when observed by microscopy (Fig. 2A and B). These embryos with the defect showed normal closure of the posterior neural tube, and the other embryonic features appeared normal except for the distortion caused by the open

anti-cleaved caspase-3 antibody-positive cells from *Trx-2*$^{-/-}$ embryos compared to wild-type embryos by immunohistochemical staining of paraffin-embedded 9.5-dpc embryos (adjacent slices of the embryos shown in panels A and B). In panels G and H, massive apoptosis in 10.5-dpc *Trx-2*$^{-/-}$ embryos can be seen compared to the wild-type embryos as visualized by anti-caspase-3 antibody staining of paraffin-embedded embryos (adjacent slices of the embryos shown in E and F). Heavy staining in the uterine tissue is not specific to cleaved caspase-3 and is due to endogenous mouse immunoglobulin G interactions with the secondary antibody.

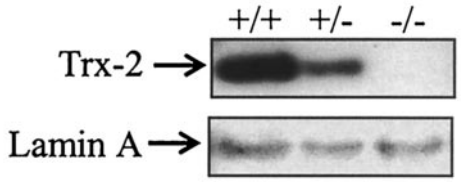

FIG. 3. Loss of Trx-2 protein in *Trx-2*$^{-/-}$ embryos. A Western blot analysis of Trx-2 protein in 30 μg of tissue homogenate from 9.5-dpc embryos is shown.

anterior neural tube. Staining of the 9.5-dpc embryos for apoptotic cells with anti-cleaved caspase-3 antibody showed a marked increase in apoptotic cells in the homozygous *Trx-2*$^{-/-}$ embryos compared to neighboring wild-type or heterozygous embryos (Fig. 2C and D). In the apoptotic cascade, procaspase-3 is cleaved after the mitochondrial cytochrome *c* release; thus, the presence of cleaved caspase-3 was used as a marker for apoptosis (27). At 10.5 dpc, we observed that surviving *Trx-2*$^{-/-}$ embryos had an open anterior neural tube and were smaller than their wild-type and *Trx-2*$^{+/-}$ littermates (Fig. 2E and F). Anti-caspase-3 staining of the 10.5-dpc embryos showed massive apoptosis in the *Trx-2*$^{-/-}$ embryos, whereas very few caspase-3 positive cells were detected in the wild-type and *Trx-2*$^{+/-}$ embryos (Fig. 2G and H). Western blot analysis of 9.5-dpc embryos verified that *Trx-2*$^{-/-}$ embryos did not have any detectable Trx-2 protein (Fig. 3).

The results of the timed pregnancies show that complete Trx-2 deficiency in the homozygous *Trx-2*$^{-/-}$ mouse is lethal early in mouse embryonic development at ca. 10.5 dpc, Theiler stage 15/16 (15). The *Trx-2*$^{-/-}$ embryos displayed an open anterior neural tube at 9.5 and 10.5 dpc, and this may contribute to their death and resorption. Other developmental processes occurring during this stage of embryogenesis, such as enlargement of the primitive heart, septum formation, and limb bud development (15), were apparently unaffected by the Trx-2 deficiency. Once closed, the anterior neural tube develops rapidly into the brain (30). An open anterior neural tube, exencephaly, is a common neural tube defect found in a wide variety of embryonic lethal mouse knockouts (14). The high prevelance of neural tube defects in mouse knockouts shows that they are probably not due to a defect specific of the neural tube closure mechanism but instead reflective of a moribund embryo (14).

The 9.5- and 10.5-dpc *Trx-2*$^{-/-}$ embryos showed increased apoptosis when stained for cleaved caspase-3. It was not clear whether this increase in apoptosis was the cause of the embryo's death prior to resorption or the beginning stages of the resorption process itself. Trx-2 has previously been reported to be essential for cell viability in vitro, with apoptosis occurring in Trx-2-deficient cells (28). This in vitro finding did not appear to carry over to the *Trx-2* knockout mouse because the *Trx-2*$^{-/-}$ embryos developed normally until day 9.5 without undergoing global apoptosis. In the developing rat embryo, it is known that at 10 to 12 dpc the mitochondria mature rapidly and begin to utilize the Krebs cycle and oxidative phosphorylation (24, 29). Although the rat and mouse have slightly different gestation times, 21 and 19 days, respectively, the embryonic developmental stages are almost identical to those of the rat, which are approximately 1 day behind the mouse (15). As the mitochondria begin to utilize oxygen at this point in embryogenesis, they would also begin to produce mitochondrial ROS. The most likely explanation for the normal appearance of *Trx-2*$^{-/-}$ embryos until 9.5 dpc is because mitochondrial ROS production is minimal prior to this stage of embryogenesis.

To further investigate the *Trx-2*$^{-/-}$ phenotype, embryonic fibroblasts were cultured from 9.5-dpc embryos. By 24 h after plating, ca. 25% of the embryos did not produce any viable fibroblasts, and these were all genotyped as homozygous *Trx-2*$^{-/-}$ (data not shown). The fibroblasts that grew were all genotyped wild-type or heterozygous *Trx-2*$^{+/-}$ (Table 1). The fibroblasts were cultured from 9.5-dpc embryos which, as previously stated, do not yet respire aerobically. When the *Trx-2*$^{-/-}$ cells are removed from the embryo and placed in routine cell culture conditions they die. These results agree with those of Tanaka et al. (28) and show the necessity of Trx-2 during cellular respiration.

Heterozygous mice have reduced protein expression of Trx-2. A decrease in *Trx-2* mRNA, measured by Northern blot analysis of liver mRNA, was observed in heterozygous *Trx-2*$^{+/-}$ mice compared to wild-type mice *Trx-2*$^{+/+}$ (Fig. 4A). Additionally, a decrease in Trx-2 protein levels, as measured by Western blot analysis, was seen in brain, liver, heart, lung, and

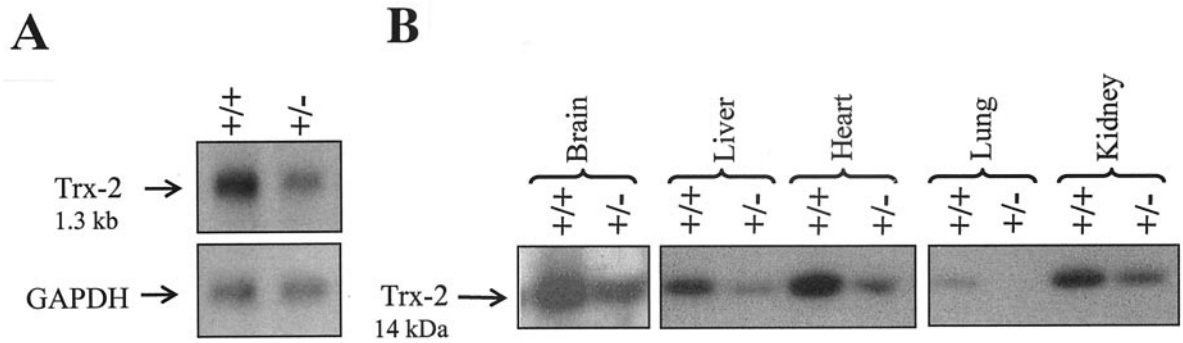

FIG. 4. Decrease of *Trx-2* transcript/Trx-2 protein in heterozygous mice. (A) *Trx-2* expression as shown by Northern blot analysis of wild-type and heterozygous *Trx-2*$^{+/-}$ mice on 2 μg of liver mRNA probed with Trx-2 and GAPDH cDNA. (B) Trx-2 protein expression in the brains, livers, hearts, lungs, and kidneys of wild-type *Trx-2*$^{+/+}$ and heterozygous mice *Trx-2*$^{+/-}$ by Western blot of 20 μg of tissue homogenate probed with α-Trx-2 rabbit polyclonal antibody.

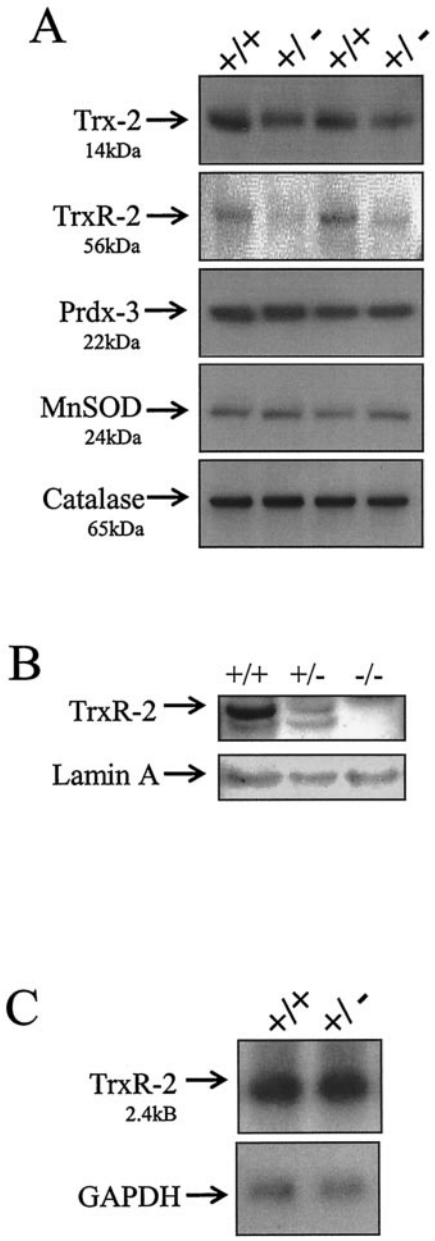

FIG. 5. Effects of decreased Trx-2 protein expression on the mitochondrial thioredoxin system, MnSOD, and catalase. (A) Western blot analysis of 20 μg of liver mitochondrial lysates from *Trx-2*$^{+/+}$ and *Trx-2*$^{+/-}$ mice. The same blot was stripped and reprobed with antibodies to TRX-2 (14 kDa), TRXR-2 (56 kDa), PRDX-3 (22 kDa), MnSOD (24 kDa), and catalase (65 kDa). (B) Western blot analysis of TrxR-2 protein in 30 μg of tissue homogenate from 9.5-dpc embryos. (C) *TrxR-2* gene expression in *Trx-2*$^{+/+}$ and *Trx-2*$^{+/-}$ mice analyzed by Northern blot with TrxR-2 and GAPDH cDNA.

kidney homogenates from heterozygous *Trx-2*$^{+/-}$ mice (Fig. 4B).

The heterozygous *Trx-2*$^{+/-}$ mice, at least up to 8 months of age, do not have a gross phenotype and do not display upregulation of other mitochondrial antioxidant proteins. To examine whether the decrease of Trx-2 protein expression in the heterozygous mice altered the expression of other mitochondrial antioxidant proteins, Western blot analysis was performed on *Trx-2*$^{+/+}$ and *Trx-2*$^{+/-}$ liver mitochondrial lysates. Trx-2 and TrxR-2 protein expression was greatly reduced in the *Trx-2*$^{+/-}$ mice, whereas Prdx-3, MnSOD, and catalase levels remained unchanged (Fig. 5A). Western blot analysis of 9.5-dpc embryos showed that *Trx-2*$^{-/-}$ embryos did not have any detectable TrxR-2 protein (Fig. 5B). The decrease in TrxR-2 protein expression was further investigated by examining gene expression. Northern blot analysis revealed that *TrxR-2* mRNA levels were not affected in Tax2$^{+/-}$ mice (Fig. 5C). Therefore, the mechanism leading to this decrease in TrxR-2 protein in response to the decrease in Trx-2 is unknown, but it appears to occur posttranscriptionally. Other members of the selenoprotein family, of which TrxR-2 is a member, have been previously been shown to be regulated posttranscriptionally by incorporation of selenium (12).

The absence of a discernible phenotype in heterozygous *Trx-2*$^{+/-}$ mice with a lethal phenotype in homozygous *Trx-2*$^{-/-}$ mice is similar to findings reported with Sod-2 knockout mice (18). Sod-2 is a mitochondrial superoxide dismutase that scavenges superoxide radical by catalytically converting it to hydrogen peroxide (18). Although heterozygous *Sod-2*$^{+/-}$ do not have a gross phenotype, they do have increased sensitivity to mitochondrial toxins, ionizing radiation, and oxygen toxicity, as well as age-related mitochondrial deficiencies (1, 2, 10, 17). Since the *Sod-2*$^{+/-}$ phenotypes were only observed under stressed conditions and the *Trx-2*$^{+/-}$ mice do not have a discernible phenotype, this suggests that mitochondrial antioxidants may be present in excess in nonmutant mice under normal conditions.

ACKNOWLEDGMENTS

We thank Loretta Barbercheck and Bob Hunter for invaluable help with the animal care and handling techniques.

This work was supported by a grant from the Arizona Disease Control Research Commission (G.P.) and NIH grants CA23074 (R.P.E.) and CA77204 (G.P.).

REFERENCES

1. **Andreassen, O. A., R. J. Ferrante, A. Dedeoglu, D. W. Alber, P. Klivenyi, E. J. Carlson, C. J. Epstein, and M. F. Beal.** 2001. Mice with a partial deficiency of manganese superoxide dismutase show increased vulnerability to the mitochondrial toxins malone, 3-nitropropionic acid, and MPTP. Exp. Neurol. **167:**189–195.
2. **Asikainen, T. M., T. T. Huang, E. Taskinen, A. L. Levonen, E. Carlson, R. Lapatto, C. J. Epstein, and K. O. Raivio.** 2001. Increased sensitivity of homozygous Sod2 mutant mice to oxygen toxicity. Free Radic. Biol. Med. **32:**175–186.
3. **Boveris, A.** 1984. Determination of the production of superoxide radicals and hydrogen peroxide in mitochondria. Methods Enzymol. **105:**429–435.
4. **Bustamante, E., J. W. Sper, and P. L. Pedersen.** 1977. A high-yield preparative method for isolation of rat liver mitochondria. Anal. Biochem. **80:**401–408.
5. **Chae, H. Z., H. J. Kim, S. W. Kang, and S. G. Rhee.** 1999. Characterization of three isoforms of mammalian peroxiredoxin that reduce peroxides in the presence of thioredoxin. Diabetes Res. Clin. Pract. **45:**101–112.
6. **Chae, H. Z., K. Robison, L. B. Poole, G. Church, G. Storz, and S. G. Rhee.** 1994. Cloning and sequencing of thiol-specific antioxidant form mammalian brain: alkyl hydroperoxide reductase and thiol-specific antioxidant define a large family of antioxidant enzymes. Proc. Natl. Acad Sci. USA **91:**7017–7021.
7. **Chae, H. Z., T. B. Uhm, and S. G. Rhee.** 1994. Dimerization of thiol-specific antioxidant and the essential role of cysteine 47. Proc. Natl. Acad Sci. USA **91:**7022–7026.
8. **Chen, Y., J. Cai, T. J. Murphy, and D. P. Jones.** 2002. Overexpressed human mitochondrial thioredoxin confers resistance to oxidant-induced apoptosis in human osteosarcoma cells. J. Biol. Chem. **277:**33242–33248.
9. **Damdimopoulos, A. E., A. Miranda-Vizuete, M. Pelto-Huikko, A. Gustafs-**

son, and G. Spyrou. 2002. Human mitochondrial thioredoxin: involvement in mitochondrial membrane potential and cell death. J. Biol. Chem. **277:**33249–33257.
10. **Epperly, M. W., C. J. Epstein, E. L. Travis, and J. S. Greenberger.** 2000. Decrease pulmonary radiation resistance of manganese superoxide dismutase (MnSOD)-deficient mice is corrected by human manganese superoxide dismutase-plasmid/liposome (SOD2-PL) intratracheal gene therapy. Radiat. Res. **154:**365–374.
11. **Gladyshev, V. N., A. Liu, S. V. Novoselov, K. Krysan, Q. A. Sun, V. M. Kryudov, G. V. Kryukov, and M. F. Lou.** 2001. Identification and characterization of a new mammalian glutaredoxin (thioltransferase), Grx2. J. Biol. Chem. **276:**30374–30380.
12. **Hadly, K. B., and R. A. Sunde.** 2001. Selenium regulation of thioredoxin reductase activity and mRNA levels in rat liver. J. Nutr. Biochem. **12:**693–703.
13. **Huang, R. P., J. X. Wu, Y. Fan, and E. D. Adamson.** 1996. UV activates growth factor receptors via reactive oxygen species. J. Cell Biol. **133:**211–220.
14. **Juriloff, D. M., and M. J. Harris.** 1999. Mini-review: toward understanding mechanisms of genetic neural tube defects in mice. Teratology **60:**292–305.
15. **Kaufman, M. H.** 1999. The atlas of mouse development. Academic Press, Inc., San Diego, Calif.
16. **Knopp, E. A., T. L. Arndt, K. L. Eng, M. Caldwell, R. C. Leboef, S. S. Deeb, and K. D. O'Brien.** 1999. Murine phospholipids hydroperoxide glutathione peroxidase: cDNA sequence, tissue expression, and mapping. Mamm. Genome **10:**601–605.
17. **Kokoszka, J. E., P. Coskun, L. A. Esposito, and D. C. Wallace.** 2001. Increased mitochondrial oxidative stress in the $Sod2^{+/-}$ mouse results in age-related decline of mitochondrial function culminating in increased apoptosis. Proc. Natl. Acad Sci. USA **98:**2278–2283.
18. **Li, Y., T. T. Huang, E. J. Carlson, S. Melov, P. C. Ursell, J. L. Olson, L. J. Noble, M. P. Yoshimura, C. Berger, P. H. Chan, D. C. Wallace, and C. J. Epstein.** 1995. Dilated cardiomyopathy and neonatal lethality in mutant mice lacking manganese superoxide dismutase. Nat. Genet. **11:**376–381.
19. **Lui, X., C. N. Kim, J. Yang, R. Jemmerson, and X. Wang.** 1996. Induction of apoptotic program in cell-free extracts: requirement for dATP and cytochrome *c*. Cell **86:**147–157.
20. **Miranda-Vizuete, A., A. E. Damdimopoulos, and G. Spyrou.** 1999. cDNA cloning, expression, and chromosomal localization of the mouse mitochondrial thioredoxin reductase gene (1). Biochim. Biophys. Acta **1447:**113–118.
21. **Miranda-Vizuete, A., A. E. Damdimopoulos, and G. Spyrou.** 2000. The mitochondrial thioredoxin system. Antioxid. Redox Signal **2:**801–810.
22. **Radi, R., J. F. Turrens, L. Y. Change, K. M. Bush, J. D. Crapo, and B. A. Freeman.** 1991. Detection of catalase in rat heart mitochondria. J. Biol. Chem. **266:**22022–22028.
23. **Salas-Vidal, E., H. Lomeli, S. Castro-Obregon, R. Cuervo, D. Escalante-Alcalde, and L. Covarrubias.** 1998. Reactive oxygen species participate in the control of mouse embryonic cell death. Exp. Cell Res. **238:**136–147.
24. **Shepard, T. H., L. A. Muffley, and L. T. Smith.** 1998. Ultrastructural study of mitochondria and their cristea in embryonic rats and primate. Anat. Rec. **252:**383–392.
25. **Simon, H. U., A. Yehia-Haj, and F. Levi-Schaffer.** 2000. Role of reactive oxygen species (ROS) in apoptosis function. Apoptosis **5:**415–418.
26. **Spyrou, G., E. Enmark, A. Miranda-Vizuete, and J. Gustafsson.** 1997. Cloning and expression of a novel mammalian thioredoxin. J. Biol. Chem. **272:**2936–2941.
27. **Susin, S. A., N. Zamzami, M. Castedo, T. Hirsch, P. Marchetti, A. Macho, E. Daugas, M. Geuskens, and G. Kroemer.** 1996. Bcl-2 inhibits the mitochondrial release of an apoptogenic protease. J. Exp. Med. **184:**1331–1341.
28. **Tanaka, T., F. Hosoi, Y. Yamguchi-Iwai, H. Nakmura, H. Masutani, S. Ueda, A. Nishiyama, S. Takeda, H. Wada, G. Spyrou, and J. Yodoi.** 2002. Thioredoxin-2 (TRX-2) is an essential gene regulating mitochondria-dependent apoptosis. EMBO **21:**1695–1703.
29. **Tanimura, T., and T. H. Shepard.** 1970. Glucose metabolism by rat embryos in vitro. Proc. Soc. Exp. Biol. Med. **135:**51–54.
30. **Theiler, K.** 1972. The house mouse. Springer-Verlag, Berlin, Germany.
31. **Van Remmen, H., and A. Richardson.** 2001. Oxidative damage to mitochondria and aging. Exp. Gerontol. **36:**957–968.
32. **Zambrowicz, B. P., G. A. Fredrich, E. C. Buxton, S. L. Lilleberg, C. Person, and A. T. Sands.** 1998. Disruption and sequence identification of 2,000 genes in mouse embryonic stem cells. Nature **392:**608–611.
33. **Zoratti, M., and I. Szabo.** 1995. The mitochondrial permeability transition. Biochim. Biophys. Acta **1241:**139–176.